

Supporting Information

Designing a Beryllium-Free Deep-Ultraviolet Nonlinear Optical Material without Structural Instability Problem

Sangen Zhao,[†] Lei Kang,^{‡,//} Yaoguo Shen,^{†,//} Xiaodong Wang,[§] Muhammad Adnan Asghar,^{†,//} Zheshuai Lin,^{*,‡}
Yingying Xu,^{†,//} Siyuan Zeng,[†] Maochun Hong,[†] and Junhua Luo^{*,†}

[†]Key Laboratory of Optoelectronic Materials Chemistry and Physics, Fujian Institute of Research on the Structure of Matter, Chinese Academy of Sciences, Fuzhou, Fujian 350002, China

[‡]Beijing Center for Crystal R&D, Key Lab of Functional Crystals and Laser Technology of Chinese Academy of Sciences, Technical Institute of Physics and Chemistry, Chinese Academy of Sciences, Beijing 100190, China

[§]Changchun Institute of Optics, Fine Mechanics and Physics, Chinese Academy of Sciences, Changchun 130033, China

^{//}University of Chinese Academy of Sciences, Beijing 100049, China

CONTENTS

Reagents	S2
Synthesis of I Powders	S2
Growth of I Crystals	S2
Single-Crystal Structure Determination	S2
Elemental Analysis	S3
Thermal Stability	S3
Second-Harmonic Generation	S3
Computational Methods	S3
Figure S1. Experimental and calculated XRD patterns of I	S5
Figure S2. DSC curves of I	S5
Figure S3. [LiAl ₂ B ₃ O ₁₀ F] _∞ single-layer.	S5
Figure S4. Density of states and partial density of states plots of I	S6
Figure S5. Dispersion curves of refractive index of I	S6
Table S1. Crystal data and structure refinement for I	S7
Table S2. Atomic coordinates and equivalent isotropic displacement parameters for I	S8
Table S3. Anisotropic displacement parameters (Å ²) for I	S9
Table S4. Selected bond distances (Å) and angles (deg.) for I	S10
References:	S11

Reagents

K₂CO₃ (99.99%), BaCO₃ (99.998%), BaF₂ (99.99%), Li₂CO₃ (99.998%), Al₂O₃ (99.999%), LiF (99.99%), and H₃BO₃ (99.998%) were purchased from Aladdin and used as received.

Synthesis of **I** Powders

Polycrystalline **I** was synthesized by the traditional solid-state reaction techniques. A mixture of K₂CO₃ 20.73 g (0.15 mol), BaCO₃ 59.20 g (0.30 mol), Li₂CO₃ 3.69 g (0.05 mol), Al₂O₃ 20.39 g (0.20 mol), LiF 2.59 g (0.10 mol), and H₃BO₃ 37.10 g (0.6 mol) was thoroughly ground, slowly heated to 773 K at a rate of 10 K/h, and then sintered at this temperature for 24 h. The products were ground thoroughly, heated to 923 K at a rate of 30 K/h, and then sintered at this temperature for 150 h with several intermediate grindings. The phase purity was confirmed by powder X-ray diffraction (XRD) analysis, which was carried out at room temperature on a Rigaku MiniFlex II diffractometer equipped with Cu K α radiation in the 2θ range of 10–70°. The measured XRD pattern well matches the calculated one based on single-crystal XRD analysis (see Figure S1).

Growth of **I** Crystals

Single crystals of **I** were grown by the top-seeded solution growth method with the flux Li₂O-BaF₂-B₂O₃ at a molar ratio of **I**:Li₂O:BaF₂:B₂O₃ = 1:4:1:3. A mixture of **I** powders, Li₂CO₃, BaF₂, and H₃BO₃ was placed into a Φ 45 \times 45 mm platinum crucible in batches and melted at 1173 K in a temperature-programmable electric furnace. The melt was held at this temperature for 24 h to ensure that it was homogenized. A platinum wire serving as a nucleation center was dipped into the melt, which was rapidly cooled to 1073 K and then allowed to cool at a rate of 2 K/h until **I** crystals crystallized on the platinum wire. The crystals were subsequently drawn out of the melt and used as the seed crystals. In the following run of growth, the crystallized temperature was firstly determined by a tentative seed crystal method. A seed crystal was attached to a platinum rod, and then slowly dipped into the melt at 20 K above the crystallized temperature. The temperature was held for 60 min to dissolve the rough surfaces of the seed crystal, and then decreased to the crystallized temperature in 5 min before the melt was allowed to cool at a rate of 0.2-1.0 K per day. When the growth finished, the crystal was drawn out of the melt and cooled down to room temperature at a rate of 20 K/h.

Single-Crystal Structure Determination

A colorless **I** crystal (0.26 \times 0.20 \times 0.13 mm³) was selected using an optical microscope for single-crystal XRD analysis. The diffraction data were collected by using graphite-monochromatized Mo K α radiation (λ = 0.71073 Å) at 298 (2) K on an Agilent SuperNova Dual diffractometer with an Atlas detector. The collection of the intensity data, cell refinement, and data reduction were carried out with the program CrysAlisPro.¹ The structure was solved by the direct method with program SHELXS and refined with the least-squares program SHELXL.² Final refinements include anisotropic displacement parameters. The structure was verified using the ADDSYM

algorithm from the program PLATON,³ and no higher symmetry was found. Details of crystal parameters, data collection, and structure refinement are summarized in Table S1. The atomic coordinates and equivalent isotropic displacement parameters are listed in Table S2. The anisotropic displacement parameters are listed in Table S3, and the selected bond distances and angles are presented in Table S4.

Elemental Analysis

The inductively coupled plasma elemental analysis of **I** was measured using a Varian Vita-Pro CCD simultaneous inductively coupled plasma-optical emission spectrometer. The crystal samples were dissolved in nitric acid at the boiling point for 1 h. The result, K:Ba:Li:Al:B = 2.79:3.10:1.91:4.16:6.28, is consistent with the compositions determined by single-crystal XRD analysis.

Thermal Stability

The thermal stability was investigated by the differential scanning calorimetric (DSC) analysis on a NETZSCH DTA404PC thermal analyzer (the DSC was calibrated with Al₂O₃) in an atmosphere of flowing N₂. About 21.2 mg **I** powders were placed into an Al₂O₃ crucible, heated at a rate of 20 K min⁻¹ from room temperature to 1373 K, and then cooled to room temperature at the same rate.

Second-Harmonic Generation

The measurements were performed with a Q-switched Nd:YAG laser at a wavelength of 1064 nm. Polycrystalline **I** samples were ground and sieved into the following particle size ranges: 0–50 μm, 50–75 μm, 75–125 μm, 125–188 μm, 188–250 μm, and 250–300 μm. Crystalline KH₂PO₄ (KDP) samples were also ground and sieved into the same particle size ranges and used as the references for second-harmonic generation (SHG) tests. The samples were pressed between glass slides and secured with tape in 1-mm thick aluminum holders containing an 8-mm diameter hole. They were then placed into a light-tight box and irradiated with the laser of 1064 nm. The intensity of the frequency-doubled output emitted from the samples was collected by a photomultiplier tube.

Computational Methods

The first-principles calculations were performed by the plane-wave pseudopotential method implemented in the CASTEP package based on the density functional theory.⁴ The ion-electron interactions were modeled by the optimized normal-conserving pseudopotentials for all elements.⁵ The generalized gradient approximation (GGA) with Perdew–Burke–Ernzerhof (PBE) functionals was adopted.⁶ The kinetic energy cutoffs of 1000 eV and Monkhorst-Pack k-point meshes⁷ with the spanning of less than 0.07/Å³ in the Brillouin zone were chosen. Based on the calculated electronic structures, the refractive indices n (and the birefringence Δn) can be obtained.

Meanwhile, the SHG coefficients d_{ij} were calculated using an expression developed by Lin *et al.*⁸ In addition, to verify the structural stability, the linear response method⁹ was employed to obtain the phonon dispersion of **I** and SBBO crystals. The certain directions in the k-points from Γ (0 0 0) to A (0 0 0.5) to H (-0.333, 0.667 0.5) to K (-0.333, 0.667, 0) to Γ (0 0 0) to Λ (0, 0.5, 0.5) to M (0, 0.5, 0) to H (-0.333, 0.667, 0.5) represent other high symmetry paths in the Brillouin Zone. Our tests reveal that the above computational parameters are sufficiently accurate for present purposes.

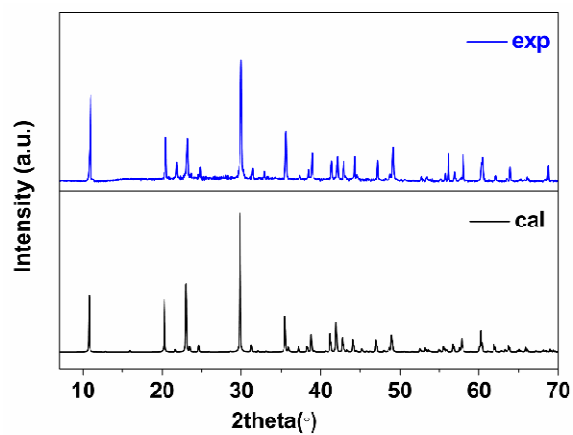


Figure S1. Experimental and calculated XRD patterns of **I**.

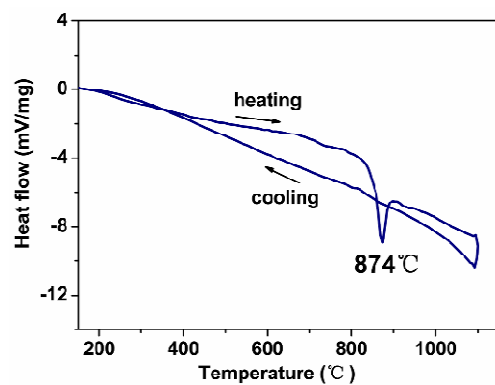


Figure S2. DSC curves of **I**.

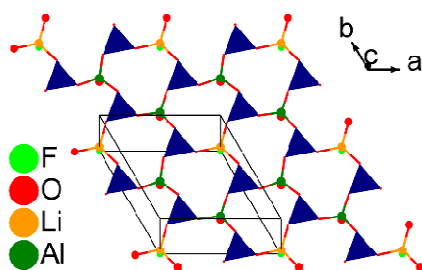


Figure S3. $[\text{LiAl}_2\text{B}_3\text{O}_{10}\text{F}]_\infty$ single-layer. Blue triangles represent $[\text{BO}_3]^{3-}$ groups.

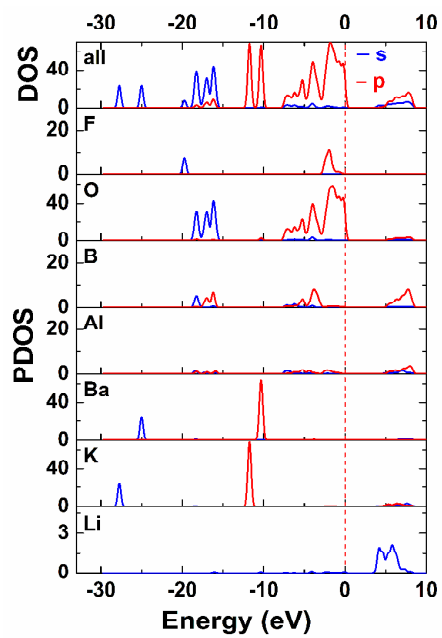


Figure S4. Density of states and partial density of states plots of I.

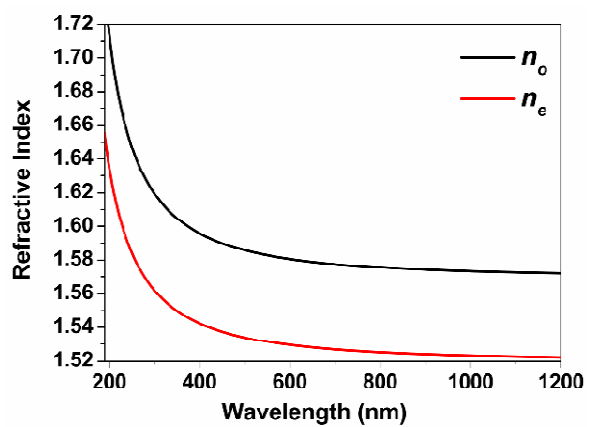


Figure S5. Dispersion curves of refractive index of I.

Table S1. Crystal data and structure refinement for I

Formula sum	$\text{K}_3\text{Ba}_3\text{Li}_2\text{Al}_4\text{B}_6\text{O}_{20}\text{F}$
Formula weight (g/mol)	1054.98
Crystal color	colorless
Crystal size/mm	$0.26 \times 0.20 \times 0.13$
Crystal system	hexagonal
Space group	$P \bar{6}2c$ (190)
$a/\text{\AA}$	8.7547(3)
$c/\text{\AA}$	16.4346(9)
$V/\text{\AA}^3$	1090.87(8)
Z	2
μ/mm^{-1}	6.190
$F(000)$	964
Data/restraints/parameters	773/0/63
$R(\text{int})$	0.0220
$\text{GOF}(F^2)$	1.089
Flack parameter	0.03(4)
Final R indices $[F_o^2 > 2\sigma(F_c^2)]^a$	$R_1 = 0.0220$, $wR_2 = 0.0524$
Final R indices (all data) ^a	$R_1 = 0.0232$, $wR_2 = 0.0534$

$$^a R_1 = \sum_o \|F_o\| - \|F_c\| / \sum_o \|F_o\| \text{ and } wR_2 = \left[\sum w(F_o^2 - F_c^2) / \sum wF_o^4 \right]^{1/2} \text{ for } F_o^2 > 2\sigma(F_c^2).$$

Table S2. Atomic coordinates and equivalent isotropic displacement parameters for I

Atom	Wyck.	Site	S.O.F.	x/a	y/b	z/c	$U [\text{\AA}^2]^a$
Ba1	6h	m..		0.01235(3)	0.31625(4)	3/4	0.01337(16)
K1	6g	.2.		0	0.29556(19)	1/2	0.0255(3)
Li1	4e	3..		0	0	0.8851(8)	0.006(3)
Al1	4f	3..		1/3	2/3	0.89627(18)	0.0120(5)
Al2	4f	3..		2/3	1/3	0.89557(17)	0.0121(5)
B1	12i	1		0.3505(8)	0.3455(7)	0.8565(5)	0.0172(15)
O1	4f	3..		2/3	1/3	0.9999(2)	0.042(3)
O2	12i	1		0.5319(4)	0.4141(4)	0.85993(16)	0.0265(8)
O3	12i	1		0.2917(4)	0.4654(5)	0.85685(18)	0.0305(8)
O4	12i	1		0.2334(5)	0.1732(5)	0.85440(18)	0.0275(7)
F1	2a	32.		0	0	1.00000	0.028(2)

^a U_{eq} is defined as one-third of the trace of the orthogonalized U_{ij} tensor.

Table S3. Anisotropic displacement parameters (\AA^2) for I

Atom	U_{11}	U_{22}	U_{33}	U_{12}	U_{13}	U_{23}
Ba1	0.0096(2)	0.0102(2)	0.0188(2)	0.00384(17)	0.00000	0.00000
K1	0.0275(9)	0.0236(5)	0.0269(8)	0.0138(5)	0.0055(4)	0.0027(2)
B1	0.022(3)	0.017(3)	0.012(3)	0.009(3)	0.003(2)	0.003(2)
F1	0.038(3)	0.038(3)	0.009(3)	0.0188(16)	0.00000	0.00000
Li1	0.005(4)	0.005(4)	0.007(6)	0.002(2)	0.00000	0.00000
Al1	0.0071(7)	0.0071(7)	0.0220(13)	0.0035(4)	0.00000	0.00000
Al2	0.0093(8)	0.0093(8)	0.0175(13)	0.0047(4)	0.00000	0.00000
O1	0.057(4)	0.057(4)	0.014(4)	0.028(2)	0.00000	0.00000
O2	0.013(2)	0.0171(16)	0.0510(17)	0.0084(19)	0.0000(14)	0.0111(13)
O3	0.0226(17)	0.015(2)	0.0573(17)	0.012(2)	-0.0177(14)	-0.0116(18)
O4	0.016(2)	0.012(2)	0.0506(16)	0.0035(15)	0.0104(16)	-0.0056(16)

Table S4. Selected bond distances (Å) and angles (deg.) for I

Ba1—O4 ⁱ	2.639(3)	K1—F1 ^{vi}	2.5876(16)
Ba1—O4 ⁱⁱ	2.639(3)	K1—O4 ^{vii}	3.024(3)
Ba1—O3 ⁱⁱⁱ	2.753(3)	K1—O4 ⁱ	3.024(3)
Ba1—O2 ^{iv}	2.801(3)	K1—O1 ^{vii}	3.0968(9)
Ba1—O2 ^v	2.801(3)	K1—O1 ^v	3.0968(9)
Ba1—O4 ⁱⁱⁱ	3.268(3)	K1—O2 ^v	3.194(3)
Li1—F1	1.889(13)	K1—O2 ^{viii}	3.194(3)
Li1—O4 ^{xvi}	1.905(5)	K1—O3 ⁱⁱⁱ	3.236(3)
Li1—O4 ⁱⁱ	1.905(5)	K1—O3 ^{ix}	3.236(3)
Li1—O4	1.905(5)	Al2—O2 ^{xviii}	1.752(3)
B1—O4	1.335(7)	Al2—O2 ^{xix}	1.752(4)
B1—O3	1.381(6)	Al2—O1	1.715(4)
B1—O2	1.390(6)	Al2—O2	1.752(3)
O4—B1—O3	119.5(4)	Al1—O3	1.736(4)
O4—B1—O2	123.7(4)	Al1—O1 ^{xviii}	1.706(4)
O3—B1—O2	116.8(4)	Al1—O3 ^{iv}	1.736(4)
		Al1—O3 ^{xi}	1.736(4)

Symmetry codes: (i) -y, x-y, 1.5-z; (ii) -y, x-y, z; (iii) x, y, 1.5-z; (iv) -x+y, 1-x, z; (v) -x+y, 1-x, 1.5-z; (vi) -x+y, -x, 1.5-z; (vii) y, x, -0.5+z; (viii) x-y, 1-y, -0.5+z; (ix) -x, -x+y, -0.5+z; (x) -1+y, x, -0.5+z; (xi) 1-y, 1+x-y, z; (xii) x-y, -y, 2-z; (xiii) 1-y, 1+x-y, 1.5-z; (xiv) 1+x-y, 1-y, 2-z; (xv) 1+x, y, 1.5-z; (xvi) -x+y, -x, z; (xvii) x-y, 1-y, 2-z; (xviii) 1-y, x-y, z; (xix) 1-x+y, 1-x, z.

References:

- (1) CrysAlisPro, Version 1.171.36.28; Agilent Technologies: Santa Clara, CA, **2013**.
- (2) Sheldrick, G. M. *Acta Crystallogr. A* **2008**, *64*, 112.
- (3) Spek, A. L. *J. Appl. Crystallogr.* **2003**, *36*, 7.
- (4) (a) Kohn, W.; Sham, L. J. *Phys. Rev.* **1965**, *140*, A1133; (b) Payne, M. C.; Teter, M. P.; Allan, D. C.; Arias, T. A.; Joannopoulos, J. D. *Rev. Mod. Phys.* **1992**, *64*, 1045; (c) Clark, S. J.; Segall, M. D.; Pickard, C. J.; Hasnip, P. J.; Probert, M. J.; Refson, K.; Payne, M. C. *Z. Kristallogr.* **2005**, *220*, 567.
- (5) Rappe, A. M.; Rabe, K. M.; Kaxiras, E.; Joannopoulos, J. D. *Phys. Rev. B* **1990**, *41*, 1227.
- (6) Perdew, J. P.; Zunger, A. *Phys. Rev. B* **1981**, *23*, 5048.
- (7) Monkhorst, H. J.; Pack, J. D. *Phys. Rev. B* **1976**, *13*, 5188.
- (8) (a) Lin, J.; Lee, M. H.; Liu, Z. P.; Chen, C. T.; Pickard, C. J. *Phys. Rev. B* **1999**, *60*, 13380; (b) Lin, Z. S.; Jiang, X. X.; Kang, L.; Gong, P. F.; Luo, S. Y.; Lee, M. H. *J. Phys. D-Appl. Phys.* **2014**, *47*, 253001.
- (9) Baroni, S.; de Gironcoli, S.; Dal Corso, A.; Giannozzi, P. *Rev. Mod. Phys.* **2001**, *73*, 515.